Available online at www.sciencedirect.com
SCIENCE DIRECT
Journal of Molecular Catalysis B: Enzymatic 41 (2006) 110–116
JOURNAL OF MOLECULAR CATALYSIS B: ENZYMATIC
www.elsevier.com/locate/molcatb

Enantioselectivity of resolved Δ and Λ orthoruthenated 2-phenylpyridine complexes $[Ru(o\text{-}C_6H_4\text{-}2\text{-}py)(LL)_2]PF_6$ (LL = bpy and phen) toward glucose oxidase

Ekaterina V. Ivanova [a,1], Igor V. Kurnikov [b], Andreas Fischer [c], Larissa Alexandrova [d], Alexander D. Ryabov [e,*]

[a] *Department of Chemistry, Moscow State University, 119899 Moscow, Russia*
[b] *Department of Environmental and Occupational Health, University of Pittsburgh, Pittsburgh, PA, USA*
[c] *Inorganic Chemistry, Department of Chemistry, Royal Institute of Technology, S-100 44 Stockholm, Sweden*
[d] *Instituto de Investigaciones en Materiales, UNAM, Circuito Exterior s/n, Ciudad Universitaria, Mexico, DF 04510, Mexico*
[e] *Department of Chemistry, Carnegie Mellon University, 4400 Fifth Av., Pittsburgh, PA 15213, USA*

Received 13 January 2006; received in revised form 11 May 2006; accepted 19 May 2006
Available online 27 June 2006

Abstract

Cyclometalated 2-phenylpyridine complexes $[Ru^{II}(o\text{-}C_6H_4\text{-}2\text{-}py)(LL)_2]PF_6$, LL = 2,2′-bipyridine (**1**) and 1,10-phenanthroline (**2**) were resolved into Δ and Λ enantiomers using column chromatography on SP Sephadex C-25 in the presence of (+)-2,3-dibenzoyl-*D*-tartrate. The absolute configuration of enantiomers was established using circular dichroism spectroscopy. The rate constants k_{et} for the electron transfer from reduced glucose oxidase (GO from *Aspergillus niger*) and PQQ-dependent glucose dehydrogenase (GDH) at the generated Ru^{III} species were measured by cyclic voltammetry and UV–vis spectroscopy. The electron transfer shows enantioselectivity. In the case of GO, the bell-shaped pH profile for the ratio k_Λ/k_Δ has a maximum at pH 7 (k_Λ/k_Δ equals 3.4 and 3.9 for **1** and **2**, respectively), but its inversion is observed at pH around 5 and 9. The k_Λ/k_Δ ratio equals 2.0 for **2** and GDH at pH 7. The results of theoretical modeling of biological electron transfer for GO using functional docking Monte-Carlo simulations are presented and analyzed together with the experimental observations.

Keywords: Ruthenium; Cyclometalated compounds; X-ray crystallography; Glucose oxidase; PQQ glucose dehydrogenase; Electron transfer; Functional docking Monte-Carlo simulation

1. Introduction

Recently we described a variety of biorganometallic applications of orthometalated Ru^{II} and Os^{II} derivatives of 2-phenylpyridine and 2-(4-tolyl)pyridine [1]. These octahedral compounds (Scheme 1) are capable of rapid electron exchange with the active sites of redox enzymes such as glucose oxidases [2–5], several peroxidases [2,6], PQQ-dependent dehydrogenases (PQQ, pyrroloquinoline quinone) [7,8], and laccase [9]. All complexes in Scheme 1 may exist as pure Δ and Λ enantiomers with the central metal chirality [10]. We [11] and others [12] have previously shown enantioselectivity of the electron transfer between redox enzymes and organometallic compounds with the planar chirality such as 1,2-disubstituted ferrocenes. Here, we describe that similar enantioselectivity can be achieved for organometallic Ru^{II} complexes with the element of central metal chirality. This effect is shown to occur in catalysis by both glucose oxidase from *Aspergillus niger* and PQQ-dependent glucose dehydrogenase in the presence of resolved complexes **1** and **2** (by column chromatography on SP Sephadex C-25 using (+)-2,3-dibenzoyl-*D*-tartrate). Enantiomerically pure Δ and Λ forms of **1** were previously obtained by different approaches, viz. by using an anionic $\{[MnCo(oxalate)_3]^-\}_n$ network [13] or reacting Δ and Λ enantiomers of $[Ru(bpy)_2py_2]X$ with 2-phenylpyridine in ethylene glycol at 120 °C, i.e. under rather harsh conditions [14]. X-ray crystallographic characterization of racemic complex **1** is also reported in this work, as well as the

* Corresponding author. Tel.: +1 412 268 6177; fax: +1 412 268 1061.
E-mail address: ryabov@andrew.cmu.edu (A.D. Ryabov).
[1] Present address: Faculty of Life Sciences, Michael Smith Building, Oxford Road, Manchester M13 9PT, United Kingdom.

1381-1177/$ – see front matter © 2006 Elsevier B.V. All rights reserved.
doi:10.1016/j.molcatb.2006.05.008

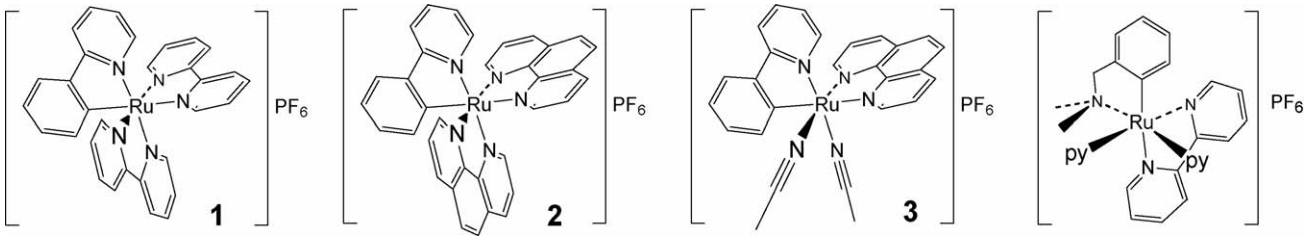

Scheme 1. Examples of Ru^{II} metalacycles used as redox partners of enzymes.

results of theoretical analysis on intrinsic reasons of the reported enantioselectivity in catalysis by GO.

2. Results and discussion

2.1. Resolution of ruthenium(II) complexes *1* and *2*

Successful resolution of a number of ruthenium(II) polypyridyl complexes of charge +2 into Δ and Λ enantiomers using column chromatography with a SP Sephadex C-25 carrier and eluents containing chiral anions has been described by several groups of workers [15,16]. The charge of orthoruthenated cations **1** and **2** of similar structure equals +1. Nevertheless, the same routine using (+)-2,3-dibenzoyl-*D*-tartrate for creating a pair of diastereomers can be used. However, low solubility of **1** and **2** does not allow to scale up the separation. Complexes **1** and **2** are intensively colored species and therefore the course of separation has been followed visually. The separation length for **1** and **2** on a column of 2.5 cm in diameter was different, viz. 40 and 15 cm for **1** and **2**, respectively, implying that bulkier complexes are easier to separate as observed for complexes of the type $[Ru(R_2\text{-bpy})_3]^{2+}$ and $[Ru(phen)_3]^{2+}$ [15]. The (+)-2,3-dibenzoyl-*D*-tartrate as a counter-ion in all diastereomers was replaced by PF_6^- using ion-exchange chromatography on a Dowex 1-X2 (AG 1-42) resin.

The electronic spectra of both pairs of enantiomers were similar. The CD spectra of the Δ and Λ forms of complex **1** were practically identical to the spectra reported previously [14]. The CD spectra of the **2** enantiomers are shown in Fig. 1. It should be emphasized that the CD spectra of the **1** and **2** enantiomers match those of complexes of the $[Ru(R_2\text{-bpy})_3]^{2+}$ type. The absolute configuration of $[Ru(Me_2\text{-bpy})_3]^{2+}$ was established by the X-ray crystallography [15]. We failed to prepare a good quality crystal of enantiomerically pure complexes and therefore the absolute configuration of enantiomers **1** and **2** was assigned by comparing their CD spectra with those reported for a variety of $[Ru(R_n\text{-bpy})_3]^{2+}$ complexes. A positive Cotton effect around 300 nm is observed for the the Λ form of $[Ru(Me_2\text{-bpy})_3]^{2+}$ [15]. We assume that the Λ configuration for **1** or **2** should be assigned to those stereoisomers that have a positive Cotton effect at the same wavelength. Complexes **1** and **2** are characterized by large extinction coefficients in the visible region of spectrum [2]. This is why we could not measure precisely the values of optical rotation of the isolated stereoisomers. The signs of rotation were only determined. The Λ and Δ forms of **1** and **2** rotate the polarized light clockwise and anticlockwise, respectively. A milder separation procedure and comparison of our data with the data reported previously [14] both suggest that the optical purity of the materials reported here is not lower than 60% ee (Fig. 2).

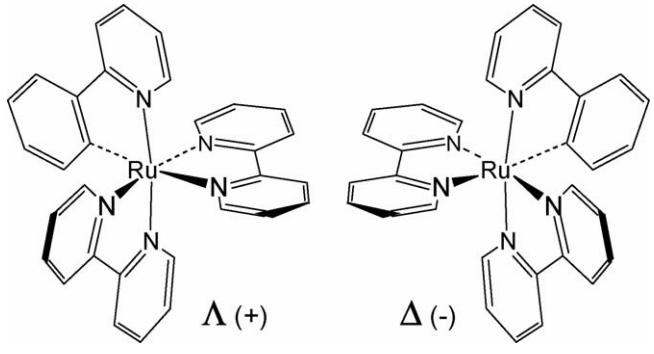

Fig. 1. Λ and Δ stereoisomers of complex **1**.

2.2. X-ray structural characterization of racemic complex *1*

X-ray crystallographic data for complexes such as **1**–**3** has previously been reported [2,13,17]. The objective of this study was to determine the absolute configuration of **1** by X-ray crystallography. Unfortunately, this goal was not reached and the data reported here refer to the racemic complex **1**. The ORTEP diagram is presented in Fig. 3. Crystallographically, all three ligands are identical implying that bound to Ru^{II} five nitrogen

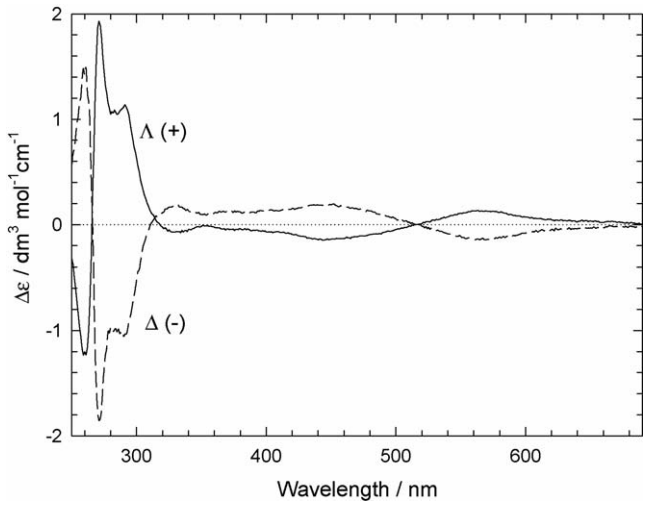

Fig. 2. CD spectra of resolved Λ and Δ stereoisomers of complex **2** (5×10^{-5} M) recorded in MeOH.

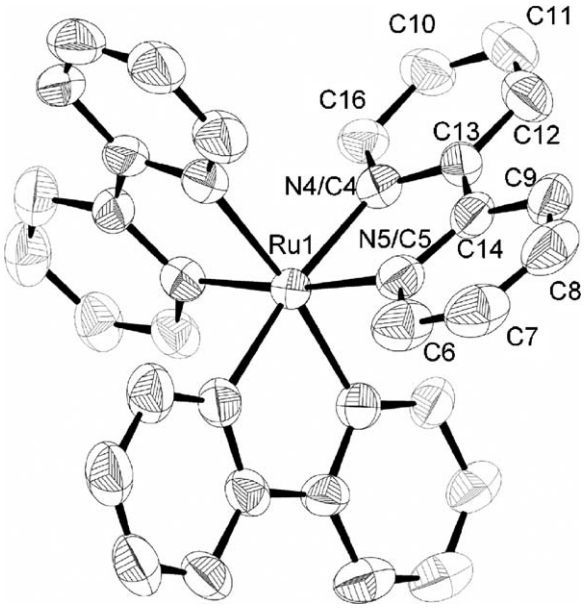

Fig. 3. ORTEP diagrams for racemic complex **1** (H atoms and the PF_6^- counter ion are not shown for clarity). Ellipsoids represent a 50% probability level. Average bond length Ru-N/C: 2.068 Å.

atoms are indistinguishable from carbon. We are sure that the data was not collected for $[Ru(bpy)_3](PF_6)_2$ because there is only one PF_6^- anion per one ruthenium center in the complex. In general, the structure of complex **1** is similar to related orthoruthenated molecules [2,17] and complexes of the $[Ru(bpy)_3](PF_6)_2$ type [18–20].

2.3. Reactivity of oxidized complexes *1* and *2* with respect to reduced glucose oxidase and PQQ-dependent glucose dehydrogenase

The reactivity of racemic ruthena(II)cycles **1** and **2** toward reduced glucose oxidase GO(red) was studied by cyclic voltammetry [2]. The reactivity of Δ and Λ enantiomers of **1** and **2** toward GO in buffered aqueous solutions was investigated similarly. Representative data obtained for complex **1** is demonstrated in Fig. 4. As seen, the electrocatalysis involving the Λ enantiomer is more efficient than that by the Δ enantiomer. The electrochemical data was interpreted in terms of Scheme 2 (the stoichiometric coefficients are omitted for clarity). At pH 7, the second-order rate constants k_{et} for the oxidation of the reduced enzyme by the electrochemically generated Ru^{III} species (step 3) were calculated using the routine of Bourdillon et al. [21]; the corresponding data obtained for complexes **1** and **2** are shown in Table 1.

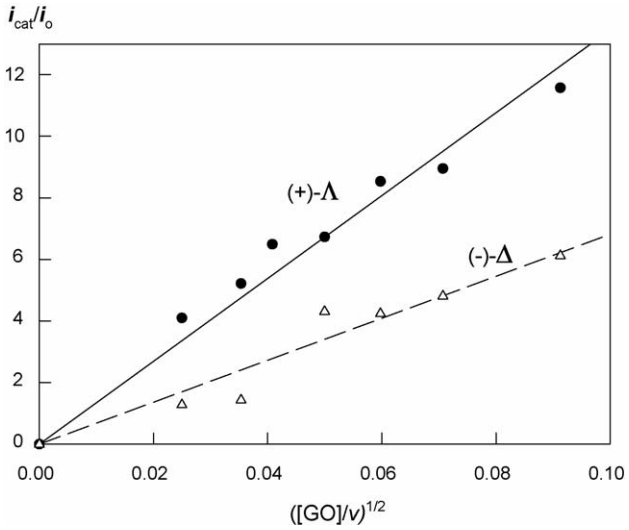

Fig. 4. The current ratio i_{cat}/i_o against $([GO]/v)^{1/2}$ (v is sweep rate, $V\,s^{-1}$) for the system Ru^{II}–*D*-glucose–GO: [**1**] = 5.0×10^{-5} M, [*D*-glucose] = 0.1 M, [GO] = 1×10^{-6} M, pH 7 (50 mM phosphate), 25 °C.

Table 1
Rate constants for the oxidation of reduced active sites of GO and GDH by electrochemically generated enantiomers of Δ and Λ Ru^{III} complexes in 50 mM phosphate buffer, pH 7.0, 25 °C, $[Ru^{II}] = 5 \times 10^{-5}$ M, [*D*-glucose] = 0.1 M, [Enzyme] = 1×10^{-6} M

Complex	Configuration	Enzyme	k_{et} ($M^{-1}\,s^{-1}$)	k_Λ/k_Δ
1	Λ (+)	GO	$(1.54 \pm 0.05) \times 10^7$	3.42
1	Δ (−)	GO	$(4.49 \pm 0.02) \times 10^6$	
2	Λ (+)	GO	$(5.68 \pm 0.03) \times 10^6$	3.88
2	Δ (−)	GO	$(1.45 \pm 0.07) \times 10^6$	
2	Λ (+)	GDH	$(8.79 \pm 0.09) \times 10^5$	2.00
2	Δ (−)	GDH	$(4.39 \pm 0.05) \times 10^5$	

The data in Table 1 reveal that the reactivity of the Δ and Λ enantiomers of ruthena(III)cycles **1** and **2** toward reduced GO is different. The enantioselectivity factor, i.e. the ratio of the rate constants k_Λ/k_Δ, is slightly lower than 4. The k_Λ/k_Δ ratio exceeds appreciably that reported for Δ and Λ enantiomers of $[Os(4,4'\text{-}Me_2bpy)_3]^{2+}$ [22]. The Δ enantiomer of $[Os(4,4'\text{-}Me_2bpy)_3]^{2+}$ is only by a factor of 1.39 is more reactive than Λ at pH 7 and 25 °C. The enantioselectivity factor is also higher than that for planar chiral *S*- and *R*-2-methylferrocene carboxylic acid, for which the relevant k_S/k_R ratio was 1.7 (pH 7) [11].

As of other enzymes [23], the reactivity of GO depends strongly on pH. Interestingly, pH profiles for GO are substrate-dependent implying that different group of atoms of the active site of GO can be involved in the catalysis [24]. Therefore it was interesting to see how the enantioselectivity factor depends

$$\textit{D}\text{-glucose} + \text{Enzyme(ox)} \rightarrow \textit{D}\text{-}\delta\text{-gluconolactone} + \text{Enzyme(red)} \quad (1)$$

$$\text{Enzyme(red)} + Ru^{III} \rightarrow \text{Enzyme(ox)} + Ru^{II} \quad (k_{et}) \quad (2)$$

$$Ru^{II} - e \rightarrow Ru^{III} \quad \text{(electrode)} \quad (3)$$

Scheme 2. Adopted mechanism of electrocatalysis by glucose oxidase and glucose dehydrogenase.

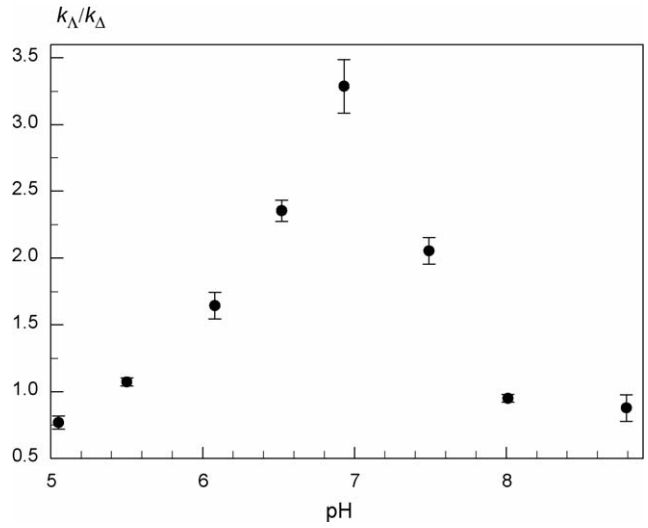

Fig. 5. pH dependence of the enantioselectivity factor k_Λ/k_Δ for GO-catalyzed reduction of Ru^{III} derived from Δ and Λ enantiomers of **1**. [39] = 5.0×10^{-5} M, [*D*-glucose] = 0.3 M, [GO] = 5×10^{-9} M, 50 mM phosphate buffer, 25 °C.

on pH in the range 5–9 for Δ and Λ forms of **1**. These experiments were performed spectrophotometrically. Complex **1** was oxidized *in situ* into its Ru^{III} form by H_2O_2 in the presence of horseradish peroxidase and the reduction of Ru^{III} into Ru^{II} by GO(red) was followed by monitoring an increase in absorbance at 494 nm due to regeneration of the stronger absorbing Ru^{II} species. The results obtained by UV–vis spectroscopy (Fig. 5) agree with the data obtained cyclic voltammetry, i.e. the Λ enantiomer is appreciably more reactive at pH 7. The pH dependence of the k_Δ/k_Λ ratio is pseudo bell-shaped (Fig. 5). At extreme pH, viz. 5 and 9, there is inversion of the enantioselectivity factor and the reactivity of the Δ enantiomer exceeds that of Λ, the k_Δ/k_Λ ratio being 1.30 and 1.14 at pH 5.05 and 8.9, respectively. Intuitively, this phenomenon is easy to rationalize. Changes of pH affect subtly the geometry and electrostatic environment of the chiral active site of GO [25]. These changes differentially influence the interaction of Λ and Δ enantiomers of **1** with GO resulting in different averaged distances between Ru^{III} and $FADH_2$ of reduced GO. Therefore the rates of electron transfer vary as well [26]. It will be shown below that these qualitative considerations find a support in theoretical modeling of biological electron transfer performed using functional docking Monte-Carlo simulations [27].

Similar experiments were performed for the system **1/2**–*D*-glucose–PQQ-dependent GDH. This enzyme belongs to a family of PQQ-dependent oxidizing biocatalysts, which has been discovered about two decades ago [28,29]. They use electron acceptors other than dioxygen (cytochromes *c*, small blue-copper proteins, or an internal heme *c* group) to perform the reoxidation [28,29]. Previously, several ferrocene [30,31] and ruthenium [7,8] species were introduced as mediators of PQQ-dependent alcohol and glucose dehydrogenases. Here, we show that GDH is capable of discriminating Δ and Λ enantiomers of complex **1**. The electrochemical data for GO and GDH were obtained and analyzed similarly. The catalytic cycles for GO and GDH are also identical. Scheme 2 is valid for the both enzymes. The corresponding rate constants k_Λ and k_Δ calculated using the formalism of Bourdillon et al. [21] are shown in Table 1. The ratio k_Λ/k_Δ equals 2.0 and it is lower than that for glucose oxidase. The absolute values of the rate constants are also lower for GDH as compared with GO.

2.4. Functional docking for glucose oxidase

The flavin adenine dinucleotide redox prosthetic group of GO (FAD) is deeply buried inside the protein [25]. Substrates access FAD through a deep funnel-shaped pocket. Complexes **1** or **2** are unable to reach FAD, and the bimolecular electron transfer is likely to occur in a "rapid-equilibration" regime. The latter implies that redox partners have a low probability to react during a lifetime of encounter complex between two molecules [27]. The rate constant for bimolecular electron transfer between GO(red) and Ru^{III} can be expressed as a Boltzmann-weighted average of the rate constants in all protein/mediator complexes [27].

$$k_2^{ET} \approx p_i k_i^{ET} = \frac{\exp(-E_i/k_B T)}{\sum_i \exp(-E_i/k_B T)} k_i^{ET} \quad (4)$$

here, p_i, E_i, and k_i^{ET} are the probability of formation, the complex formation (interaction) energy, and electron-tunneling rate constant for each particular complex. The rate constants k_i^{ET} depend strongly on the geometry of protein/mediator complexes, particularly on the distance between reduced $FADH_2$ and Ru^{III}. In addition, an orientation of **1** or **2** and a chemical nature of "bridging" protein residues that mediate the electronic interactions between the $FADH_2$ and Ru^{III} also play a role [32]. The observed values of k_2^{ET} (which should be related to k_{et} in Scheme 2) depend on a small fraction of intermolecular complexes (but not necessary on a single complex) that have both high rates of electron tunneling k_i^{ET} and low intermolecular interaction energy E_i. The functional Docking Monte-Carlo simulation [27] allows to identify and probe preferentially configurations with high k_i^{ET}. For each simulation step k_i^{ET} is estimated using the PATHWAYS model [33] and E_i is estimated using a finite-difference solution of the Poisson-Boltzmann equation [27]. When the PATHWAYS model [33] is applied to GO and **1**, the corresponding donor and acceptor groups with delocalized donor and acceptor electronic states should be specified. Hartree-Fock calculations of **1** showed that a 1e state that accepts electron from $FADH_2$ is localized primarily on Ru and the cyclometalated ring (see Fig. 6). Therefore this fragment was selected as an acceptor group.

"Functional Docking" simulations generated a set of GO/**1** encounter complexes with high k_i^{ET} and low E_i. A typical active configuration is presented in Fig. 7. Here the metalated ring of Λ enanatiomer is in a non-bonding contact with Tyr68 that in turn interacts with $FADH_2$. A transition from the Λ to Δ enantiomer does not change electronic coupling, but the computed electrostatic energy increases by ~2 kcal mol^{-1}. This increase may account for a more than 10-fold difference in the electron transfer rates for the Δ and Λ forms (see Eq. (4)). Averaged

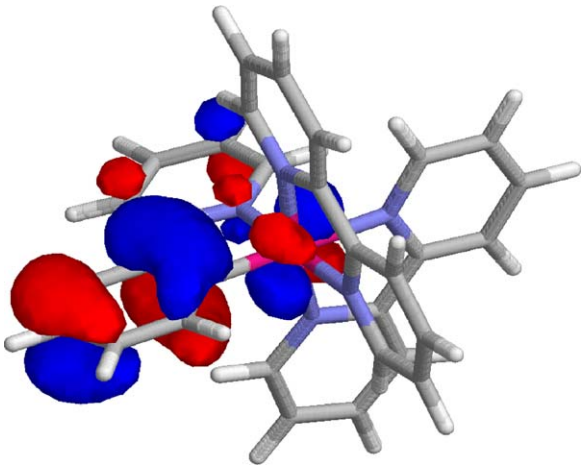

Fig. 6. Isodensity surfaces of highest occupied molecular orbital of compound **1** (Ru^{II} total complex charge +1e). This one electronic state accepts electron from $FADH_2$ during oxidation of reduced GO.

changes of k_2^{ET} for the Λ and Δ enantiomers have been computed as described elsewhere [27] by using a routine involving (i) conversion of the Λ into Δ enantiomer in every point of the Monte-Carlo trajectory, (ii) computing resulting changes of the electrostatic energies, and (iii) performing the same operation on the Monte-Carlo trajectory of Δ enanatiomer. The computed ratio of the rate constant for Λ and Δ enantiomers was 2.6 consistent with a maximal value of ca. 4.0 observed in the experiment.

In conclusion, "Functional Docking" simulations are applied for a qualitative interpretation of the observed difference in the reactivity of two enantiomers of $[Ru(o\text{-}C_6H_4\text{-}2\text{-}py)(LL)_2]PF_6$ (LL = bpy and phen). High rates electron transfer dictate a specific orientation of the mediators in productive complexes and thus two enantiomers in their most favorable configurations will have different energies accounting for different rates of oxidation of GO(red).

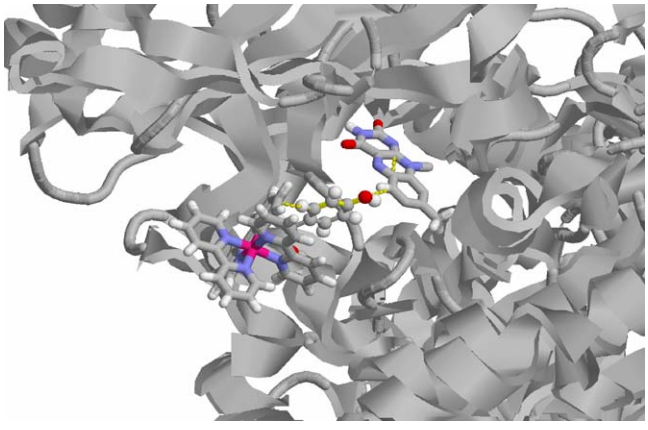

Fig. 7. Interaction complex between GO and the Λ enantiomer of **1** generated using functional docking siumulations. Yellow line show the best electronic coupling path (computed with PATHWAYS model) between $FADH_2$ and metalated ring of compound **1** (acceptor group in PATHWAYS calculations).

3. Experimental

3.1. Materials

Racemic complexes **1** and **2** were obtained as described elsewhere [2]. *D*-(+)-Glucose was obtained from ICN Biomedicals. PQQ-dependent glucose dehydrogenase was purified from *Erwinia* sp. 34-1 (specific activity 12 U mg^{-1}) and used as a solution in 0.02 M phosphate buffer containing 10% glycerol [34]. Sephadex SP C-25 was purchased from Pharmacia. Dowex 50w-X2 (AG 1-42) was from Serva. The eluent was prepared by neutralization of 50 mM solution of (+)-2,3-dibenzoyl-*D*-tartaric acid (Fluka) by two equivalents of sodium hydroxide. The pH of the final solution (8.0) was controlled by a pH meter. Chloroform and acetonitrile were from Khimmed. KPF_6 was from Fluka. Glucose oxidase from *Aspergilius niger* (EC 1.1.3.4) has activity 250 U mg^{-1} was purchased from ICN and used as received.

3.2. Methods

Electronic spectra were obtained on a Shimadzu U-160A spectrophotometer. Signs of optical rotation were determined using an Autopol II polarimeter (Rudolf Research Analytical). CD spectra were obtained using a Jasco J-715 instrument. Electrochemical measurements were performed on a PC-interfaced potentiostat-galvanostat IPC-4 (Institute of Physical Chemistry, RAS, Moscow, Russia). A three-electrode scheme was used with a BAS working glassy carbon electrode, saturated calomel or Ag/AgCl reference electrodes, and auxiliary Pt electrode. Before measurements the working electrode was polished with a diamond paste and rinsed with ethanol and distilled water. Anodic peak currents (i_o) were obtained from cyclic voltammograms in the absence of enzymes. Catalytic currents (i_{cat}) were obtained in the presence of GO or GDH and *D*-glucose. The rate constants k_{et} were calculated from the slopes of linear plots of the ratio (i_{cat}/i_o) against $([enzyme]/v)^{1/2}$ (v is the scan rate) as originally described elsewhere [21] and applied in our previous studies [2,4,5,11,35].

Measurements of rates of reduction of Ru^{III} compounds derived from complexes **1** and **2** by UV–vis spectroscopy were carried out as described below. Solutions of Ru^{III} compounds were made *in situ*, just before measurements. To 5×10^{-5} M solution of **1** or **2** in phosphate buffer (0.01 M) an aliquote of H_2O_2 was added to achieve the concentration of H_2O_2 in the reaction solution of 5×10^{-5} M. Oxidation of Ru^{II} into Ru^{III} was initiated by adding a solution of horseradish peroxidase (HRP, Sigma). The final concentration of HRP in solution was 3×10^{-9} M. The course of oxidation was monitored by measuring the absorbance of the Ru^{II} species at 494 and 480 nm for **1** and **2**, respectively. The glucose oxidase-catalyzed oxidation of *D*-glucose by thus generated Ru^{III} species was followed by monitoring the absorbance increase at the same wavelengths due to formation of Ru^{II} after addition of GO and *D*-glucose to the reaction mixtures containing Ru^{III}. The final concentrations of GO and *D*-glucose equal 5×10^{-9} and 0.03 M, respectively. Initial rates were for individual enantiomers were calculated from

the slopes of the absorbance versus time plots. Data in Fig. 4 is the ratio of the initial rates obtained for Λ and Δ enantiomers.

3.3. Resolution of *1* and *2*

A column (2.5 cm × 50 cm) was loaded with Sephadex SP C-25 equilibrated with 50 mM of sodium (+)-2,3-dibenzoyl-*D*-tartrate (pH 8). Complexes **1** and **2** (1 mg mL^{-1}) were dissolved in MeOH and 500 μL of the solution were brought on the column equilibrated with 0.05 M solution of (+)-2,3-dibenzoyl-*D*-tartrate. Elution was performed with the same solution that contained up to 10% of MeOH. A degree of resolution of enantiomers was controlled visually. Complete resolution of diastereomers was observed. The corresponding fractions were separated and treated with an equal volume of chloroform. The organic layer was separated and the organic solvent was evaporated to dryness. (+)-2,3-Dibenzoyl-*D*-tartrate was removed chromatographically by eluting the correspondent diastereomer with a mixture of 1 M aqueous KPF_6 and acetonitrile (7:3, v/v) from the anion exchange resin Dowex 1-X2 (AG 1-42). Then the ruthenium complex was extracted into the equal volume of the chloroform and evaporated to dryness using a rotary evaporator.

3.4. X-ray studies

Crystal data, data collection, and refinement parameters are given in Table 2. Diffraction intensity data were collected on a Bruker-Nonius KappaCCD. The structures were solved by direct methods and completed by subsequent difference Fourier syntheses and refined by full matrix least-squares procedures on F^2. The symmetry requires all three ligands to be equivalent, thus suggesting a complete disorder of the ligands over all possible orientations. Crystallographic data have been deposited with the Cambridge Crystallographic Data Center as Supplementary Publication No. CCDC-287408.

Table 2
Crystallographic data and summary of data collection and structure refinement for *rac*-**1**

Formula	$C_{31}H_{24}F_6N_5PRu$
fw	712.59
Diffractometer	Bruker-Nonius KappaCCD
Wavelength (Å)	0.71073
Crystal system	Trigonal
Space group	*R*-3*c*
T (K)	299(2)
a (Å)	13.751(1)
c (Å)	51.417(1)
V (Å^3)	8584(1)
Z	12
D_{calc} (g cm^{-3})	1.903
θ Range (deg) for data collection	4.30–26.4
$N_{measured}$	15868
$N_{independent}$	1947
R	0.0757
wR_2	0.1894
GOF	1.020
Largest difference between peak and hole (e Å^{-3})	1.03/−0.69

3.5. Computational details

Hartree–Fock calculations of the reduced and oxidized state of **1** (formal charges +1 and +2) were performed in 3-21G basis set using GAUSSIAN-98 [36]. Partial atomic charges were derived from the electronic density obtained in Hartree–Fock calculations using Merz–Kollman procedure [37]. Functional Docking Monte-Carlo simulations were done using a HARLEM program [38]. Finite-difference solution of the Poisson–Boltzmann equation for GO electrostatic filed used 241 × 241 × 241 grid, 100 mM ionic strength. Steric interactions between GO and **1** were computed using the exclusion volume of GO expanded on the 241 × 241 × 241 grid. PATHWAYS calculations of donor/acceptor electronic interactions used a decay constant for intermolecular non-bonded constant of $\beta_{NB} = 0.9$ Å^{-1} as in ref. [27]. Other PATHWAYS model parameters are the same as in ref. [33].

Acknowledgements

We thank Dr. Rolandas Meškys and Prof. Dr. Valdas Laurinavičius (Institute of Biochemistry, Vilnius, Lithuania) for providing samples of PQQ glucose dehydrogenase. L.A. is greatful to CONACyT (34293-E and 40135-Q) for financial support.

References

[1] A.D. Ryabov, Adv. Inorg. Chem. 55 (2004) 201.
[2] A.D. Ryabov, V.S. Sukharev, L. Alexandrova, R. Le Lagadec, M. Pfeffer, Inorg. Chem. 40 (2001) 6529.
[3] M.E. Davydova, V.S. Kurova, M.V. Sukhacheva, M.B. Kupletskaya, A.D. Ryabov, A.I. Netrusov, Vestn.Mosk. Un-ta, Ser. 2 Khim. 43 (2002) 366.
[4] A.D. Ryabov, V.S. Soukharev, L. Alexandrova, R. Le Lagadec, M. Pfeffer, Inorg. Chem. 42 (2003) 6598.
[5] A.D. Ryabov, V.S. Kurova, E.V. Ivanova, R. Le Lagadec, L. Alexandrova, Anal. Chem. 77 (2005) 1132.
[6] I.S. Alpeeva, V.S. Soukharev, L. Alexandrova, N.V. Shilova, N.V. Bovin, E. Csöregi, A.D. Ryabov, I.Y. Sakharov, J. Biol. Inorg. Chem. 8 (2003) 683.
[7] R. Le Lagadec, L. Rubio, L. Alexandrova, R.A. Toscano, E.V. Ivanova, R. Meškys, V. Laurinavicius, M. Pfeffer, A.D. Ryabov, J. Organomet. Chem. 689 (2004) 4820.
[8] R. Le Lagadec, L. Alexandrova, H. Estevez, M. Pfeffer, V. Laurinavicius, J. Razumiene, A.D. Ryabov, Eur. J. Inorg. Chem., (2006), in press.
[9] A.S. Vilesov, S.A. Kurzeev, T.V. Fedorova, E.V. Stepanova, O.V. Koroleva, A.D. Ryabov, Manuscript in preparation.
[10] A. von Zelewsky, Stereochemistry of Coordination Compounds, John Wiley & Sons, Chichester, New York, 1996.
[11] A.D. Ryabov, Y.N. Firsova, V.N. Goral, E.S. Ryabova, A.N. Shevelkova, L.L. Troitskaya, T.V. Demeschik, V.I. Sokolov, Chem. Eur. J. 4 (1998) 806.
[12] S.J. Sadeghi, G. Gilardi, G. Nicolosi, A.E.G. Cass, J. Chem. Soc. Chem. Commun. (1997) 517.
[13] M. Brissard, M. Gruselle, B. Malezieux, R. Thouvenot, C. Guyard-Duhayon, O. Convert, Eur. J. Inorg. Chem. (2001) 1745.
[14] M. Brissard, O. Convert, M. Gruselle, C. Guyard-Duhayon, R. Thouvenot, Inorg. Chem. 42 (2003) 1378.
[15] T.J. Rutherford, P.A. Pellegrini, J. Aldrich-Wright, P.C. Junk, F.R. Keene, Eur. J. Inorg. Chem. (1998) 1677.
[16] N.C. Fletcher, F.R. Keene, J. Chem. Soc. Dalton Trans. (1999) 683.

[17] A.D. Ryabov, R. Le Lagadec, H. Estevez, R.A. Toscano, S. Hernandez, L. Alexandrova, V.S. Kurova, A. Fischer, C. Sirlin, M. Pfeffer, Inorg. Chem. 44 (2005) 1626.
[18] D.P. Rillema, D.S. Jones, H.A. Levy, J. Chem. Soc. Chem. Commun. (1979) 849.
[19] M. Biner, H.B. Buergi, A. Ludi, C. Roehr, J. Am. Chem. Soc. 114 (1992) 5197.
[20] D.P. Rillema, D.S. Jones, C. Woods, H.A. Levy, Inorg. Chem. 31 (1992) 2935.
[21] C. Bourdillon, C. Demaille, J. Moiroux, J.-M. Savéant, J. Am. Chem. Soc. 115 (1993) 2.
[22] Y. Nakabayashi, K. Nakamura, M. Kawachi, T. Motoyama, O. Yamauchi, J. Biol. Inorg. Chem. 8 (2003) 45.
[23] A. Fersht, Structure and Mechanism in Protein Science: A Guide to Enzyme Catalysis and Protein Folding, Freeman, New York, 1999.
[24] R. Wilson, A.P.F. Turner, Biosens. Bioelectron. 7 (1992) 165.
[25] H.J. Hecht, H.M. Kalisz, J. Hendle, R.D. Schmid, D. Schomburg, J. Mol. Biol. 229 (1993) 153.
[26] C.C. Moser, J.M. Keske, K. Warncke, R.S. Farid, P.L. Dutton, Nature 355 (1992) 796.
[27] Z.-X. Liang, I.V. Kurnikov, J.M. Nocek, A.G. Mauk, D.N. Beratan, B.M. Hoffman, J. Am. Chem. Soc. 126 (2004) 2785.
[28] J.A. Duine, J. Biosci. Bioeng. 88 (1999) 231.
[29] J.A. Duine, in: J. Reedijk, E. Bouwman (Eds.), Bioinorganic Catalysis, Marcel Dekker Inc., New York, 1999, 563.
[30] J. Razumiene, R. Meskys, V. Gureviciene, V. Laurinavicius, M.D. Reshetova, A.D. Ryabov, Electrochem. Commun. 2 (2000) 307.
[31] J. Razumiene, A. Vilkanauskyte, V. Gureviciene, V. Laurinavicius, N.V. Roznyatovskaya, Y.V. Ageeva, M.D. Reshetova, A.D. Ryabov, J. Organomet. Chem. 668 (2003) 83.
[32] M.D. Newton, Chem. Rev. 91 (1991) 767.
[33] D.N. Beratan, J.N. Betts, J.N. Onuchic, Science 252 (1991) 1285.
[34] L. Marcinkeviciene, I. Bachmatova, R. Semenaite, R. Rudomanskis, G. Brazenas, R. Meskiene, R. Meskys, Biotechnol. Lett. 21 (1999) 187.
[35] V.S. Soukharev, A.D. Ryabov, E. Csöregi, J. Organomet. Chem. 668 (2003) 75.
[36] M.J. Frisch, G.W. Trucks, H.B. Schlegel, G.E. Scuseria, M.A. Robb, J.R. Cheeseman, V.G. Zakrzewski, J.A. Montgomery, Jr. , R.E. Stratmann, J.C. Burant, S. Dapprich, J.M. Millam, A.D. Daniels, K.N. Kudin, M.C. Strain, O. Farkas, J. Tomasi, V. Barone, M. Cossi, R. Cammi, B. Mennucci, C. Pomelli, C. Adamo, S. Clifford, J.W. Ochterski, G.A. Petersson, P.Y. Ayala, Q. Cui, K. Morokuma, N. Rega, P. Salvador, J.J. Dannenberg, D.K. Malick, A.D. Rabuck, K. Raghavachari, J.B. Foresman, J. Cioslowski, J.V. Ortiz, A.G. Baboul, B.B. Stefanov, G. Liu, A. Liashenko, P. Piskorz, I. Komaromi, R. Gomperts, A. Martin, D.J. Fox, T. Keith, M.A. Al-Laham, C.Y. Peng, A. Nanayakkara, M. Challacombe, P.M.W. Gill, B. Johnson, C.-L. Chen, L.L. Wong, J.L. Andres, C. Gonzalez, M. Head-Gordon, E.S. Replogle, J.A. Pople, Gaussian Inc., Pittsburgh, PA (2002).
[37] B.H. Besler, K.M. Merz Jr., P.A. Kollman, J. Comp. Chem. 11 (1990) 431.
[38] I.V. Kurnikov, M.G. Kurnikova, W. Wenzel, http://www.kurnikov.org/harlem_download/, Pittsburgh, 2005.